AGU PUBLICATIONS

Global Biogeochemical Cycles

Key Points:
- Land use and land cover change are more important than climate in modifying land carbon uptake
- When integrated to the year 2100 or 2300, indirect effects of land use on carbon are larger than direct effects
- Current land use carbon fluxes should be multiplied by 2.6 to account for future loss of natural carbon cycle sinks

Supporting Information:
- Supporting Information S1
- Figure S1
- Figure S2
- Figure S3
- Figure S4
- Figure S5
- Figure S6
- Figure S7
- Figure S8

Correspondence to:
N. M. Mahowald,
mahowald@cornell.edu

Interactions between land use change and carbon cycle feedbacks

Natalie M. Mahowald[1] (iD), James T. Randerson[2], Keith Lindsay[3], Ernesto Munoz[3], Scott C. Doney[4] (iD), Peter Lawrence[3] (iD), Sarah Schlunegger[1,5], Daniel S. Ward[1,5] (iD), David Lawrence[3], and Forrest M. Hoffman[6] (iD)

[1]Department of Earth and Atmospheric Sciences, Cornell University, Ithaca, New York, USA, [2]Department of Earth System Science, University of California, Irvine, California, USA, [3]Climate Dynamics Division, National Center for Atmospheric Research, Boulder, Colorado, USA, [4]Marine Chemistry and Geochemistry, Woods Hole Oceanographic Institution, Woods Hole, Massachusetts, USA, [5]Now at the Program in Atmospheric and Oceanic Science, Princeton University, Princeton, New Jersey, USA, [6]Climate Change Science Institute, Oak Ridge National Laboratory, Oak Ridge, Tennessee, USA

Abstract Using the Community Earth System Model, we explore the role of human land use and land cover change (LULCC) in modifying the terrestrial carbon budget in simulations forced by Representative Concentration Pathway 8.5, extended to year 2300. Overall, conversion of land (e.g., from forest to croplands via deforestation) results in a model-estimated, cumulative carbon loss of 490 Pg C between 1850 and 2300, larger than the 230 Pg C loss of carbon caused by climate change over this same interval. The LULCC carbon loss is a combination of a direct loss at the time of conversion and an indirect loss from the reduction of potential terrestrial carbon sinks. Approximately 40% of the carbon loss associated with LULCC in the simulations arises from direct human modification of the land surface; the remaining 60% is an indirect consequence of the loss of potential natural carbon sinks. Because of the multicentury carbon cycle legacy of current land use decisions, a globally averaged amplification factor of 2.6 must be applied to 2015 land use carbon losses to adjust for indirect effects. This estimate is 30% higher when considering the carbon cycle evolution after 2100. Most of the terrestrial uptake of anthropogenic carbon in the model occurs from the influence of rising atmospheric CO_2 on photosynthesis in trees, and thus, model-projected carbon feedbacks are especially sensitive to deforestation.

1. Introduction

Human land use and land cover change (LULCC) contributes to anthropogenic climate change, accounting for approximately 10–15% of the atmospheric increase in carbon dioxide (CO_2) concentrations [*Ciais et al.*, 2013a, 2013b] and for about 40% of the total radiative forcing including other heat-trapping gases [*Ward et al.*, 2014]. In addition to the effects of deforestation and harvesting on CO_2 emissions, LULCC also changes the surface albedo and biophysical properties of the land surface [e.g., *Feddema et al.*, 2005; *Jackson et al.*, 2008; *Bonan*, 2008; *DeNoblet-Ducoudre et al.*, 2012; *Brovkin et al.*, 2013; *Myhre et al.*, 2013], increases emissions of methane and nitrous oxide, and alters aerosol emissions [e.g., *Foley et al.*, 2005; *Heald and Spracken*, 2015; *Unger*, 2014; *Ward et al.*, 2014].

Because of the long lifetime of CO_2 perturbations in the ocean-atmosphere system [*Archer et al.*, 2009], over the next several centuries, the impact of the cumulative carbon emissions will dominate the forcing of global temperature change [*Allen et al.*, 2009]. Because terrestrial ecosystems represents a significant sink of anthropogenic CO_2 (currently ~25% of total emissions) [*Ciais et al.*, 2013a, 2013b, *LeQuere et al.*, 2009], conversion of land from natural to managed ecosystems reduces the capacity of the land biosphere to take up anthropogenic CO_2 in the future. This loss of a future sink is referred to as a potential indirect carbon flux from LULCC [*Gasser and Ciais*, 2013; *Gitz and Ciais*, 2003; *Pongatz et al.*, 2009]. The potential indirect carbon flux from LULCC has been identified as important in studies extending through 2100 [*Gasser and Ciais*, 2013; *Gitz and Ciais*, 2003, *Pongatz et al.*, 2009, 2010]. The relative value of mitigation options focused on land use CO_2 emissions versus fossil fuel CO_2 emissions could change in climate policies (i.e., more emphasis on reducing emissions from deforestation and forest degradation) if the indirect carbon fluxes from LULCC were included. However, there have not been any coupled-carbon-climate model studies assessing the magnitude of indirect effects of LULCC, comparing their impact with the magnitude of the climate-carbon feedback, or assessing long-term changes over a period of several centuries. Multicentennial simulations beyond 2100 can

provide important information about feedbacks in the coupled-carbon-climate system and the long-term stability of the Earth system in response to the 21st century decisions regarding energy use [*Boucher et al.*, 2012; *Frolicher and Joos*, 2010; *Randerson et al.*, 2015].

Here, for the first time, we use simulations from a full-complexity Earth system model to isolate the influence of land use and land cover change (LULCC) on the evolution of the land carbon flux in simulations that extend from 1850 to 2300. We report estimates for the largest forcing scenario—Representative Concentration Pathway 8.5 or RCP8.5 [*Hurtt et al.*, 2011; *van Vuuren et al.*, 2011; *Meinshausen et al.*, 2011]—extended to 2300. The gain of the carbon cycle-climate feedback is largest for scenarios with high atmospheric carbon dioxide levels [e.g., *Friedlingstein et al.*, 2006], although new studies have argued that permafrost feedbacks may have a larger impact at lower RCP trajectories [*MacDougall et al.*, 2012]. The RCP8.5 scenario we evaluate represents a business as usual scenario that is currently tracking observed trends in fossil fuel emissions and represents a possible future that is likely without stringent climate mitigation [*van Vuuren et al.*, 2011]. Since RCP8.5 generates a considerable climate-carbon feedback and, concurrently, produces some changes in land cover associated with agricultural expansion, it is a useful scenario for comparing climate and land use impacts on the terrestrial carbon budget. We describe the model and methodology in section 2. In section 3.1 we quantify the influence of LULCC in reducing the natural carbon sinks in the future (indirect carbon fluxes), and how that amplifies the direct CO_2 emissions from LULCC [e.g., *Gasser and Ciais*, 2013; *Pongatz et al.*, 2009; *Gitz and Ciais*, 2003; *Hansis et al.*, 2015]. We then compare the size of the LULCC feedbacks to climate and carbon dioxide fertilization feedbacks in the model. In a following step we consider how LULCC changes the evolution of the coupled-carbon-climate feedback and separate the modification of this feedback into components arising from CO_2 fertilization and climate change [e.g., *Arora et al.*, 2013; *Friedlingstein et al.*, 2006]. Finally, we use these simulations to evaluate how the CO_2 fluxes from land use occurring in 2015 will influence land carbon stocks in the long term.

2. Methods

2.1. Model Description

We used the Community Earth System model (CESM version 1) at $1° \times 1°$ resolution with ocean and land biogeochemistry for our analysis [*Hurrell et al.*, 2013; *Lindsay et al.*, 2014]. This model includes full-complexity atmosphere, land, and ocean components [*Danabasoglu et al.*, 2012; *Lawrence et al.*, 2012a; *Neale et al.*, 2013], as well as terrestrial and marine biogeochemistry [*Keppel-Aleks et al.*, 2013; *Lindsay et al.*, 2014; *Long et al.*, 2013, *Moore et al.*, 2013, *Randerson et al.*, 2015; *Thornton et al.*, 2009]. Spin-up of the CESM is a multistep process whereby the physical climate is spun up first, then the land and the ocean are spun up with fixed atmospheric carbon dioxide concentrations, and finally a 1000 year control simulation is conducted, as described in *Lindsay et al.* [2014]. The simulations for this paper branch from this control run at year 151, similar to the climate change scenario simulations submitted to the Climate Model Intercomparison Project phase 5 (CMIP5) [*Taylor et al.*, 2009].

Transient land cover is prescribed over the historical and future time period through 2100 using the RCP8.5 scenario [*Hurtt et al.*, 2011], converted into plant functional types (pfts) appropriate for implementation into this model [*Lawrence et al.*, 2012a, 2012b]. After 2100, the land use conversion is assumed to stop (i.e., the distribution of plant functional types remains constant), while harvesting is maintained at a constant rate. In this model there are 15 natural vegetation pfts and 2 crop pfts; vegetation carbon is separately calculated for each type while litter, soil carbon, and coarse woody debris are shared among all pfts within the same grid cell [*Oleson et al.*, 2013]. For the bulk of the simulations conducted here, only grid cell averages were saved as output from the model, and thus no vegetation level diagnostics are available.

Atmospheric composition, including CO_2 and aerosols, influences the Earth system in two primary ways: (1) through interacting with radiation and (2) through modifying biogeochemical exchange with the terrestrial biosphere and ocean. We isolate the impact of physical climate change (greenhouse gases and aerosols interacting with atmospheric radiation) and LULCC on land carbon stocks in our experimental design. All four of the simulations in our analysis have the terrestrial biosphere and ocean exchanging with a prescribed transient anthropogenic chemical composition (e.g., CO_2 rises from 285 ppm in 1850 to 1962 ppm in 2300). In two of the simulations, LULCC modifies terrestrial carbon fluxes (these are denoted as "with LULCC"), and in two others, land cover remains fixed at 1850 values (these are denoted as "without LULCC"). For each

set of simulations with and without LULCC, rising anthropogenic atmospheric greenhouse gases and aerosols interact with the radiation scheme (denoted as "Coupled") in one simulation and remain temporally invariant at 1850 levels in another simulation (denoted as "No anthro"). Table 1 lists the four simulations used in this study. The simulations with land use are identical to those used in *Randerson et al.* [2015].

This four-way experimental design yields simulations with and without LULCC, and with and without physical climate change, allowing us to separate the impacts of physical climate change and LULCC on land carbon stocks (Table 1). The simulations follow the historical carbon dioxide trajectory from 1850 to 2005, the RCP8.5 from 2005 to 2100 [*van Vuuren et al.*, 2011], and the Extended Concentration Pathway (ECP8.5) from 2100 to 2300 [*Meinshausen et al.*, 2011; *Meehl et al.*, 2013]. Nitrogen deposition increases until 2100 and then is held constant in all four simulations following *Lamarque et al.* [2010, 2011]. Please note that because of the biophysical response of plants to rising CO_2, there is a small amount of climate change in the No anthro case [e.g., *Swann et al.*, 2016].

Note that although *Lawrence et al.* [2012b] modified the harvesting rates input to the CESM to better reproduce the original estimates from *Hurtt et al.* [2011], these modifications were not incorporated into the simulations conducted for CMIP5 and thus were not used here or in other analyses using the same model configuration [*Lindsay et al.*, 2014; *Randerson et al.*, 2015]. Our estimates of harvest carbon loss are thus about twice as high as estimates from the forcing model [*Hurtt et al.*, 2011] as described in *Lawrence et al.* [2012b], and the impact of this on our conclusions is discussed more in section 4.

In addition, we present analysis of several sensitivity simulations (Table 1). The normal output of CESM used for the CMIP5 simulations archives only grid box average vegetation carbon [*Lawrence et al.*, 2012b; *Lindsay et al.*, 2014; *Randerson et al.*, 2015]. For some of our analysis, our goal was to explore the relative role of tree plant functional types versus other plant functional types, and thus we conducted additional 1 year time slice simulations, which branched off the long runs to provide pft level carbon pool information [*Oleson et al.*, 2013]. We conducted these simulations for four different 1 year time slices (1850, 2005, 2100, and 2300) for the coupled simulation without LULCC (Table 1) and for the 2300 time period for the other three cases (same case names but with suffix "pft" in Table 1). These 1 year branching simulations were entirely consistent with the longer simulations used in this study.

Additional sensitivity studies span the historical and RCP8.5 time period (but not extending to 2300), with boundary conditions fixed at 1865 levels (Table 1). These preindustrial sensitivity studies are (1) PI_NDEP (nitrogen deposition on land and ocean), (2) PI_AEROSOLS (anthropogenic aerosols), and (3) PI_OZONE (tropospheric and stratospheric ozone). For each of these simulations, input data sets described in the simulation name stay constant at the 1865 values and thus do not change from preindustrial levels. The resulting changes in the land-to-air fluxes for the historical time period and the 20th century (Table S1) suggest that the impact of LULCC is more important than changes in nitrogen deposition, aerosols, or ozone and thus justify the focus of this paper on LULCC.

2.2. Estimation of Carbon Effects of Land Use Conversion and Harvesting

Land use and land cover change can directly release carbon to the atmosphere through decomposition and fire and also impact the evolution of the carbon stocks on land over a period of decades to centuries [e.g., *Ciais et al.*, 2013a, 2013b; *Gasser and Ciais*, 2013; *Gitz and Ciais*, 2003, *Pongatz et al.*, 2009]. The goal here is to present a methodology to understand the relative contribution of direct versus indirect carbon stock changes in explaining the total change in land carbon between two simulations, one with LULCC and another without, and to be able to assign the carbon lost to the time of the conversion. To this end, we present a simple conceptual model of the impact of LULCC on carbon stocks and evaluate the size of each component. We consider the direct effect of land use conversion and harvesting on carbon, as well as a potential indirect impact, which is an interaction of changes in LULCC with climate, rising CO_2, and nitrogen deposition (see Figure 1; we use some of the nomenclature from *Gitz and Ciais* [2003] and *Pongatz et al.* [2009], but the details of our calculation are different). Note that there are many different approaches used in the literature for reporting land carbon stock changes, and thus we try to be clear here which processes we are including [e.g., *Houghton*, 2003; *Gasser and Ciais*, 2013; *Lawrence et al.*, 2012b; *Hansis et al.*, 2015]. The direct fluxes are by definition the change in carbon stocks that occur during 1 year from the conversion of natural lands to managed lands. For changes in pft (e.g., land conversion from forested to croplands) these fluxes are

Table 1. Case Names and Scenarios for Simulations, Indicating Transient (*T*) or Fixed at Preindustrial Values (1865) for the Simulations[a]

Case Name	CO$_2$ for Biogeochemistry	CO$_2$, Greenhouse Gases, Aerosols for Climate	LULCC	Output	Time Period
		Base Cases			
Coupled with LULCC	Transient	Transient	Transient	Standard	1850–2300
Coupled without LULCC	Transient	Transient	1865	Standard	1850–2300
No Anthro with LULCC	Transient	1865	Transient	Standard	1850–2300
No Anthro without LULCC	Transient	1865	1865	Standard	1850–2300
		Sensitivity Studies			
Coupled without LULCC-pft	Transient	Transient	1865	Pft level output	1850, 2005, 2100, and 2300
Coupled with LULCC-pft	Transient	Transient	Transient	Pft level output	2100
No Anthro with LULCC-pft	Transient	1865	Transient	Pft level output	2100
No Anthro without LULCC-pft	Transient	1865	1865	Pft level output	2100
PI-AEROSOLS	Transient	Transient CO$_2$, NDEP, and ozone, 1865 aerosols	Transient	Standard	1850–2100
PI-OZONE	Transient	Transient CO$_2$, aerosols, and NDEP, 1865 ozone	Transient	Standard	1850–2100
PI_NDEP	Transient	Transient CO$_2$, NDEP, and ozone, 1865 NDEP	Transient	Standard	1850–2100

[a]The type of output (either standard grid-average or pft-specific information), as well as the time period for the simulations is also included. More details are in section 2.1.

output from the model, while for harvesting these fluxes are not output from the model, and thus we must estimate these, as described below (equation (1)).

In CESM, land use conversion and harvesting can occur within the same grid cell, and thus, it is difficult to separate the direct and indirect changes in carbon stocks specifically for land conversion and harvesting and attribute them to the time of conversion. These two processes operate in a similar manner in that conversion of natural lands to managed land results in a direct loss of carbon for the fraction of land that is affected (Figure 1). The harvest carbon flux occurs in crops or harvested land area and consists mostly of recycled carbon (Figure 1: green line), although carbon also accumulates in product pools. There is also a loss of a potential carbon sink in managed systems, as harvesting reduces future carbon uptake in both croplands and managed forests (Figure 1). For each of these managed pfts we separate the direct carbon loss due to the conversion from indirect carbon loss due to the loss of a natural carbon sink.

We define the direct carbon change (ΔDC) as the carbon in Community Land Model (CLM) emitted directly to the atmosphere during conversion, within the first year of the transition (i.e., the changed carbon in leaf and live and dead stem carbon pools) [*Lawrence et al.*, 2012b]. Components of vegetation that are left on site and that decompose more slowly, including wood, over subsequent years to decades are referred to as the Quasi-Direct Carbon stock change (ΔQDC). ΔQDC is not archived to the output file but is important over the timescales investigated in this study (decades to centuries) [*Houghton*, 2003; *Lawrence et al.*, 2012b]. The ΔQDC carbon changes are not usually included in the calculations for direct or indirect changes in carbon [e.g., *Lawrence et al.*, 2012b], although in some approaches they are considered [*Houghton*, 2003; *Gasser and Ciais*, 2013]. We calculate ΔDC for wood harvest carbon changes due to conversion from a primary forest to a managed forest or the conversion from natural lands to crops according to

$$\Delta DC_v[x, y, t_c] = f_v[x, y, t_c] * V_v[t] / V_m * VegC_m[x, y, t_c] * EF_v \tag{1}$$

The ΔDC carbon increment is calculated at every grid box and time t_c where $f_v[x,y,t_c]$ is the fraction of the land in a grid box converted from natural lands (pft *v*) to crops or pasture (with units of fraction per year) and $VegC_m$ [*t*] is the above ground carbon in vegetation averaged across the grid box (*m*, for the mean grid box value). In CESM, this conversion is calculated separately for each pft. To simplify the problem, here we aggregate these pfts to consider only two aggregated vegetation types—tree and nontree vegetation types—and calculate separately a $f_v[x,y,t_c]$, for deforestation and for loss of nontree natural lands to crops. To account for the different amount of carbon in these two aggregated categories of vegetation in our simple
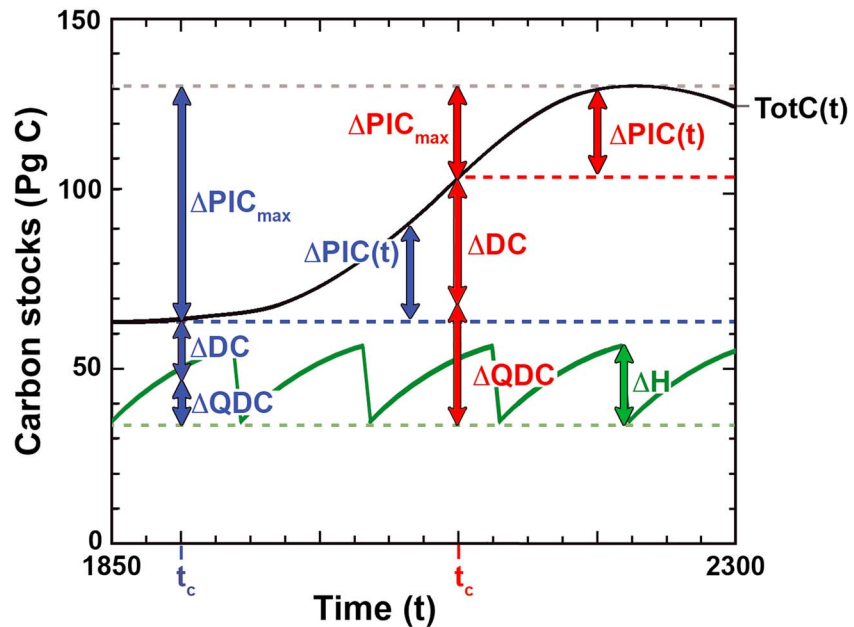
Figure 1. Schematic illustrating direct (ΔDC), *quasi-direct* (ΔQDC), and potential indirect land carbon inventory changes [ΔPIC(t)] due to land use conversion or conversion to harvested land that occurs at a grid box (x,y) at time of conversion (t_c). The evolution of the natural land carbon stock with time under higher CO_2 levels and climate change is schematically shown as the bold black line (TotC(t)). The carbon stocks at 1850 and at the peak time over the time period are shown as thin black lines. The black dotted line represents the lower carbon level that occurs after land conversion, whatever time that occurs (t_c). The direct carbon fluxes from land use (ΔDC) are estimated directly in this model and most estimates of land use conversion and carbon fluxes [e.g., *LeQuere et al.*, 2009]. In addition, there is vegetative carbon in the converted lands that is left on site in the soil or litter and which subsequently decays releasing more carbon to the atmosphere; we define this component as the quasi-direct carbon change (ΔQDC). The fraction of the vegetative carbon that is left on the land depends on the plant functional type, as discussed in section 2.2. The total column carbon (TotC[t]) is shown here to increase in time without LULCC as the natural lands take up anthropogenic carbon, and thus the land use results in an indirect change in the carbon stocks which evolves with time (ΔPIC[t_c,t]) = TotC[t] − TotC[t_c]) [*Gasser and Ciais*, 2013, *Gitz and Ciais*, 2003, *Pongatz et al.*, 2009]. Harvesting, either of crops or trees, results in a carbon flux that is largely reversible (ΔH) but causes a reduction in the total column carbon. Here conversions at two different times (t_c) are illustrated at 1860 (blue) and at 2100 (red). The maximum total carbon lost is similar in the two cases (the difference between the solid black and blue lines), but the distribution between ΔDC, ΔQDC, and ΔPIC(t) is different. The maximum amount of potential indirect carbon lost (ΔPIC$_{max}$) can be used to estimate the amplification factor by which direct carbon fluxes should be multiplied to obtain the true impact of land use conversion on the land carbon inventory. Section 2.2 describes the mathematical terms in more detail.

estimation method, we include a term representing the ratio of the amount of carbon stored in vegetation type v, relative to the average amount of vegetation carbon in the grid cell ($V_v[t]/V_m$). For simplicity, we use globally averaged values at each time, which ignores important spatial and temporal variability.

The information for how much vegetation is stored in each vegetation type is not available in the default output from CESM (only the grid cell average is available) but is calculated from extra simulations conducted as sensitivity studies for four different 1 year time slices (1850, 2005, 2100, and 2300) for the simulation with climate change but without LULCC (Table S1). The $V_v[t]/V_m$ ratio is much larger for the aggregated tree pft and increases by 10% (from 2.4 in 1850 to 2.6 in 2100; Table S1), while for the nontree pft this value is smaller and varies by less than 5% over this interval (from 0.35 in 1850 to 0.33 in 2300). We therefore neglect the temporal changes in this ratio for the nontree pfts. In CESM only leaf, live stem, and dead stem carbon are archived as components of the conversion flux, either as a flux directly emitted to the atmosphere or as a transfer to product pools. The mass of carbon associated with the conversion flux, divided by the original pool sizes of the vegetation carbon, represents the fraction of the vegetative carbon that is directly emitted to the atmosphere (emission factor or EF$_v$). Globally averaged values for EF$_v$ are 0.72 for the tree pft and 0.26 for nontree pft. The EF$_v$ values do not vary substantially over time and thus are assumed constant here (Table S1). The fluxes associated with land use conversion are archived in CESM and are compared to those estimated using this simple model (discussed in section 3.1).

The plant carbon removed by the conversion from natural lands to managed lands that is converted to litter or soil carbon (i.e., leaves, stems, or roots left on site) not directly and immediately emitted to the atmosphere (equation (1)) is the ΔQDC carbon stock change. We can also represent this quantity as a flux if we attribute this increment to the year during which the land conversion occurred and divide by a year (Figure 1):

$$\Delta QDC_v[x, y, t_c] = f_v[x, y, t_c]*V_v[t]/V_m*VegC_m[x, y, t_c]* [1 - EF_v] \qquad (2)$$

We estimate the time evolution of the loss of the potential carbon sink from the conversion at time t_c as a function of time t, the potential indirect carbon flux from vegetation type v $\Delta PIC_v[x,y,t_c,t]$, using the following equation in which TotC $[x,y,t]$ is the total grid box carbon at time t in the simulation without LULCC (Figure 1).

$$\Delta PIC_v[x, y, t_c, t] = f_v[x, y, t_c]*T_v[t]/T_m* (TotC[x, y, t] - TotC[x, y, t_c]) \qquad (3)$$

where $T_v[t]/T_m$ is the ratio amount of carbon stored in the total grid box for vegetation type v compared to the average amount of total column carbon from the sensitivity studies using the model simulation with pft level output and no LULCC. The total grid box carbon TotC$[x,y,t]$ includes the vegetation, litter, dead stems and roots, and soil carbon. The potential indirect carbon change (ΔPIC_v) often starts out at zero at the time of the land conversion t_c and increases with time [t] as the land is taking up carbon due to changes in climate, CO_2, or nitrogen deposition (TotC$[x,y,t]$−TotC $[x,y,t_c]$) (Figure 1). The increase in carbon in a natural land could occur in above ground vegetation, below ground vegetation, litter, coarse woody debris, or soil carbon pools, all of which are included in the total grid box carbon. Note that not all locations will have an increase in carbon, so that the potential indirect carbon flux could be zero or negative as well. Here again for simplicity, we consider only two aggregated pfts: tree and nontree. Based on the time slice information (from the Coupled without LULCC-pft simulation), the global average $T_v[t]/T_m$ for trees increases from 1.7 to 2.0 between 1850 and 2300 and stays relatively constant for nontree plants (0.66 at 1850 to 0.58 at 2300; Table S1).

We define the total indirect carbon change as the sum of the quasi-direct carbon and potential indirect carbon change:

$$\Delta IC_v[x, y, t_c, t] = \Delta QDC_v[x, y, t_c, t] + \Delta PIC_v[x, y, t_c, t] \qquad (4)$$

The methodology in this section relies on using vegetation carbon (at every grid box and time), total carbon (at every grid box and time), and land conversion and harvesting rates (at every grid box and time). The vegetation carbon comes from the simulation with LULCC to account for previous LULCC (and not double count previous LULCC), while the total carbon comes from the simulation without LULCC, to allow for the calculation of the potential sink. We also use time varying constants to consider the difference in vegetation carbon between tree and nontree pfts. By summing over all time, space, and the two broad vegetation types, we can recreate our estimate of the difference in total carbon that should have occurred over time due to LULCC and compare against the differences simulated in the CESM model simulations to check if our estimates are internally consistent (section 3.1). This offline analysis is necessary for separately assessing direct and indirect carbon stock changes (and fluxes) and attributing them to a specific time because these components cannot be directly estimated from the CESM model output. There are errors associated with the simplifications made in this approach, which we estimate in the supporting information, but nevertheless this approach provides useful information about long-term impacts of LULCC on the terrestrial carbon budget.

Although the change in land carbon stocks between the simulations with LULCC and without LULCC due to a transition [f_v] in grid box [x,y] is the same at 2300 no matter when the change occurs, the partitioning between indirect and direct carbon changes should be dependent on the time of the conversion from natural lands to managed lands (red versus blue cases in Figure 1). In order to consider how the proportion of direct versus indirect carbon fluxes change with time, we calculate the maximum loss over the whole time period ($\Delta IC_v[x,y,t_c,t]^{max}$; Figure 1). We can then take the ratio of the total impact of land to the direct impact to estimate the amplification factor (AF$[x,y,t_c]$) by which the modeled output direct fluxes at time t_c of land conversion carbon should be multiplied to take into account future losses in potential carbon stocks due to land use conversion at time [t_c].

$$AF_v[x, y, t_c] = \left(\Delta DC_v[x, y, t_c] + \Delta QDC_v[x, y, t_c] + \Delta PIC[x, y, t_c]_{max}\right)/\Delta DC_v[x, y, t_c] \qquad (5)$$

Thus, this methodology allows us to assign the indirect carbon changes to the time of the land use conversion, which is difficult to do otherwise.

2.3. Carbon-Climate Feedbacks and Climate Gain

Compatible fossil fuel emissions are calculated for each future scenario by allowing for a given atmospheric CO_2 concentration pathway (here the RCP8.5) and the ocean and land carbon fluxes calculated from CESM [e.g., *Arora et al.*, 2011]. Following previous studies [*Arora et al.*, 2013; *Friedlingstein et al.*, 2003], we calculate the gain in the carbon-climate system using the differences between compatible fossil fuel emissions calculated in the simulations with CO_2 and other constituents impacting the climate ($E_{coupled}$) and with no anthropogenic impact on the climate ($E_{no\ anthro}$):

$$g = \frac{E_{no\ anthro} - E_{coupled}}{E_{no\ anthro}} \qquad (6)$$

Note that our "no anthro" case excludes all greenhouse gases and aerosols, not just CO_2, and thus should be compared with caution to studies in which only the atmospheric CO_2 forcing of climate is modified.

We also use the flux-based feedback parameters to understand the relative importance of different drivers in modifying the gain, using the following equation:

$$g = -\alpha[\gamma_l + \gamma_o]/[m + \beta_l + \beta_o] \qquad (7)$$

In this approach, γ_l and γ_o represent the sensitivity of the land [*l*] and ocean [*o*] cumulative flux to changes in global mean surface temperature (units of Pg C/K), β_l and β_o are the sensitivity of the land and ocean cumulative flux to changes in atmospheric CO_2 (Pg C/ppm), and α is the change in global surface air temperature in response to changes in atmospheric CO_2 (K/ppm) [*Arora et al.*, 2013; *Friedlingstein et al.*, 2006; *Friedlingstein et al.*, 2003]. The atmospheric CO_2 value of *m* is 2.12 Pg C/ppm.

Here we consider the carbon-climate feedbacks in simulations with LULCC and without LULCC and thus need more consideration of the parameters. The carbon dioxide fertilization effect on land (β_l) and the climate impact on land carbon (γ_l) are defined as

$$\beta_l = \Delta C_{no\ anthro}/\Delta C_{atm} \qquad (8)$$

$$\gamma_l = \left(\Delta C_{coupled} - \Delta C_{no\ anthro}\right)/\Delta T_s \qquad (9)$$

where $\Delta C_{no\ anthro}$ is the change in land carbon inventory in the case with no anthropogenic climate change, ΔC_{atm} is the change in atmospheric CO_2 mole fraction, $\Delta C_{coupled}$ is the change in the land carbon inventory in the case including anthropogenic climate change, and ΔT_s is the global mean surface air temperature change. Normally, these are calculated in cases without LULCC [e.g., *Arora et al.*, 2013; *Friedlingstein et al.*, 2006]. If we calculate them in the cases with LULCC (defined here as β_l^* and γ_{l^*}), they include not only the sensitivity to CO_2 and climate but also the LULCC direct, quasi-direct and indirect carbon inventory changes. Using the estimated land use carbon changes (ΔDC, ΔQDC, and ΔIC) for the coupled (subscript *c*) and no anthro cases (subscript *u* for uncoupled) from section 3.2, we consider how each term impacts β_l^* and γ_l^*.

$$\beta_l^* = \left[\Delta C_{no\ anthro+LULCC}\right]/\Delta C_{atm} = \left[\Delta C_{no\ anthro} - \Delta DC - \Delta QDC - \Delta IC\right]/\Delta C_{atm} \qquad (10)$$

$$\gamma_l^* = \left[\Delta C_{coupled+LULCC} - \Delta C_{no\ anthro+LULCC}\right]/\Delta T_s$$

$$= \left[\left[\Delta C_{coupled} -, \Delta, DC_c, -, \Delta QDC_c, -, \Delta IC_c\right] - \left[\Delta C_{no\ anthro} -, \Delta DC_u, -, \Delta QDC_u, -, \Delta IC_u\right]\right]/\Delta T_s \qquad (11)$$

We also report the gain for the case with LULCC and without LULCC using equation (7), to understand how each term influences the strength of the climate-carbon feedback.

3. Results

The simulations analyzed here follow the RCP8.5 scenario, in which atmospheric CO_2 rises from 285 ppm in 1865 to 1962 ppm in 2300 (Figure S1a). This forcing causes a global mean surface air temperature increase of over 9 K, which continues to rise even after atmospheric CO_2 stabilizes during the second half of the 22nd century (Figure S1b). In CESM there is a slight cooling caused solely by LULCC [e.g., *Lawrence et al.* [2012b]; Figure S1b; Figure S2], with a magnitude similar to that reported for other models [e.g., *Brovkin et al.*, 2013; *DeNoblet-Ducoudre et al.*, 2012].
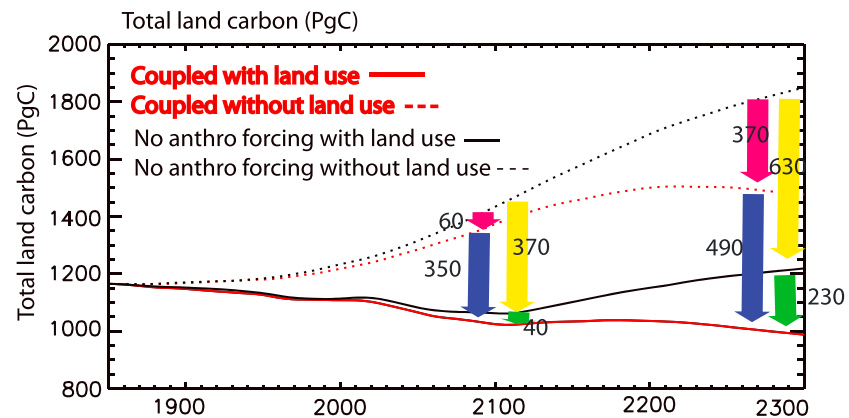
Figure 2. Time series plots from 1850 to 2300 for the historical, RCP8.5, and ECP8.5 simulations for the total column carbon (Pg C) on land. Red lines indicated simulations with changing anthropogenic forcing (especially CO$_2$) impacting climate, while black lines show the results when there is no CO$_2$ change in concentrations forcing the climate. Solid lines indicate when LULCC is changing following historical, RCP8.5, and ECP8.5 time series, while dotted lines show the results when LULCC is kept at preindustrial values. The yellow and blue arrows highlight the difference in total land carbon in simulations with and without LULCC, when there is no climate change (yellow) and when there is climate change (blue) at both 2100 and 2300. The green and the fuchsia arrows highlight the difference in total land carbon in simulations with and without climate change, when there is LULCC (green) and without LULCC (fuchsia). At 2100 and 2300, the size of the change in carbon stocks represented by the arrows in Pg C is indicated in the text written next to the arrows (also shown in Table 3, first column) and is all negative, as indicated by the downward arrow.

With rising CO$_2$, when climate change and LULCC are disabled, the land carbon inventory rises from 1200 Pg C to 1800 Pg C, an increase of 50% (Figure 2; black dotted line). With climate change included, the land carbon inventory increases from 1200 Pg C to 1500 Pg C (Figure 2; red dotted line), an increase of 25% from the combined effects of climate, CO$_2$ fertilization, and nitrogen deposition. The increase in land carbon with climate change is only half as large as the case without climate change, as expected given that climate change reduces simulated tropical net primary production and increases rates of decomposition (Figure 2; black dotted line versus red dotted line; fuchsia arrow). After 2200 the increase in land carbon inventory in the simulation with climate change flattens out because of the changes in net primary production and decomposition described above (contrast red and black dotted lines in Figure 2). The inclusion of LULCC in the simulations but without climate change yields a decrease in carbon by 2100, but a final inventory in 2300 that is similar to the inventory in 1850 (with a cumulative gain of only 50 Pg C; Table 2). Compared to the simulation without LULCC (and without climate change), the simulation with LULCC has a carbon inventory at 2300 that is about 630 Pg C lower (Figure 2; contrast black dotted line versus black solid line; yellow arrow; Table 3). Including both climate and LULCC reduces the terrestrial carbon inventory below preindustrial levels, with a final inventory in 2300 of 1000 Pg C (Table 2); this shows a further reduction of 490 Pg C due to LULCC in the case when climate is included (Figure 2; blue arrow; Table 3).

The simulated carbon cycle on land is considerably modified by LULCC; it is more important than climate in modifying the evolution of the total land carbon stocks (Figure 2 and Table 3). Indeed, in sensitivity studies conducted with this model through only 2100, LULCC is also more important than nitrogen deposition or other anthropogenic perturbations (Table S2).

The sensitivity studies looking at the pft level carbon stocks (for the simulation including climate change but no LULCC) show that most of the increase in land carbon simulated by CESM resides in the vegetation carbon pool in tree pfts. The vegetation carbon pool accounts for 72% of the total terrestrial inventory change by 2005, 81% by 2100, and 100% by 2300. During this final interval, decreases in soil carbon offset aboveground gains. Trees also are a dominant contributor to the changes in the terrestrial carbon inventory for the other simulations by 2300 (Table 3). Thus, the model system is highly sensitive to loss of forest cover by LULCC.

LULCC decreases compatible fossil fuel emissions required to stay on the RCP8.5 CO$_2$ trajectory, with an impact that is similar in size to the penalty paid for a warmer climate (Figure S1c). At 2100, LULCC and the land contribution to climate-carbon feedback reduce cumulative compatible emissions by 350 and 40 Pg C, respectively, while at 2300, these values increase to 490 and 230 Pg C, respectively (Table 2 and Table 3).

Table 2. Cumulative Carbon and Compatible Fossil Fuel Emissions for Different Cases at From 1850 to 2100 and 2300 (P gC)[a]

Case name	Cumulative Land Uptake (1850–2100) Pg C	Cumulative Land Uptake (1850–2300) Pg C	CumulativeCompatible Fossil Fuel Emissions (1850–2100) Pg C	Cumulative Compatible Fossil Fuel Emissions (1850–2300) Pg C
Coupled with LULCC	−140	−180	1730	4460
Coupled without LULCC	210	310	2080	4950
No Anthro with LULCC	−100	50	1810	5020
No Anthro without LULCC	270	690	2190	5650

[a]Case names are described in more detail in Table 1.

While much of the change in land carbon stock from LULCC is due to changes in tree carbon (Table 3), changes in soil and litter are relatively more important for the climate-carbon feedback (Table 3). LULCC does not directly impact soil carbon in CESM (Table 3), which likely represents an underestimate of the real response [*Levis et al.*, 2014; *Todd-Brown et al.*, 2013]. Indeed, although the spatial pattern of the impact of climate and LULCC on land carbon is different, in many regions the magnitude of impact is similar (Figure 3).

Without climate change or LULCC, compatible fossil fuel emissions required to stay on the prescribed atmospheric CO_2 trajectory from 1850 to 2100 are 2190 Pg C. Land climate-carbon feedbacks reduce these emissions by 40 Pg C for the case with land use (Table 2: first column: Coupled with LULCC-No Anthro with LULCC), and by 60 Pg C in the case without land use (Coupled without LULCC-No Anthro without LULCC). In contrast, LULCC reduces compatible emissions by 350 Pg C in the presence of climate change (Table 2: first column: Coupled with LULCC-Coupled without LULCC), and by 370 Pg C in the absence of climate change (No Anthro with LULCC-No Anthro without LULCC). Although there is some nonlinearity, these comparisons indicate that the direct and indirect effects of land use change were about 6–9 times more important in modifying the land contribution to compatible fossil fuel emissions than the climate-carbon feedback on land. By 2300 climate change impacts on compatible emissions cause a reduction of 230 Pg C (green arrow; Figure 2 and Table 3), while the LULCC impacts are 490 Pg C (blue arrow, Figure 2 and Table 3). This suggests land use impacts are twice as important as the climate-carbon feedback for this scenario in the CESM.

3.1. Direct and Indirect Carbon Fluxes From LULCC

To better understand the role of LULCC in modifying the carbon cycle, we consider two different approaches for examining feedbacks in the carbon-climate system in this and the following section. Here we focus on understanding the LULCC fluxes from the fully coupled simulation (the blue arrow in Figure 2). As described in the methods (section 2.2), we estimate the direct, quasi-direct, and potential indirect changes in carbon stocks, with the aim of reconstructing the temporal evolution of the total land carbon stock difference between simulations with and without LULCC (Figure 4a and Table 4). Note that although CESM does not archive detailed information about the different histories of land use (compared to, for example, the simple model of *Gasser and Ciais* [2013]), our methodology of estimating the direct fluxes from land use conversion (equation (1)) compares well to the fluxes archived from the model (Figure S3a, solid line versus dashed line). In addition, despite neglecting spatial heterogeneities in the carbon stocks of different pfts, our approach can reproduce the spatial structure of carbon loss by 2300 (Figure S4), again suggesting that our method can successfully attribute the change in carbon from LULCC between direct, quasi-direct, and potential indirect carbon stock changes.

Table 3. Total Change Due To Different Processes, and Attribution (%) in Various Land Carbon Stocks (Pg C) in Different Cases at 2300 Versus 1850, Using the Values in Table 2 or Figure 2 for the Case Names Described in Table 1[a]

Case	Total Change in Land Carbon (1850–2300)	Vegetation Carbon (%)	Tree Vegetation carbon (%)	Soil, Litter, and Coarse Woody Debris Carbon (%)
Climate impact with LULCC	−230	23	23	77
Climate impact without LULCC	−370	42	42	58
LULCC with climate	−490	96	100	4
LULCC without climate	−630	91	93	9

[a]Climate impact with LULCC = Coupled with LULCC-No Anthro with LULCC (green arrow; Figure 2). Climate impact without LULCC = Coupled without LULCC-No Anthro without LULCC (fuchsia arrow; Figure 2). LULCC with climate = Coupled with LULCC-Coupled without LULCC (blue arrow; Figure 2). LULCC without climate = No Anthro with LULCC-No Anthro without LULCC (yellow arrow; Figure 2). The results in this table come from the model results from the base cases (column 2) and the sensitivity studies with pft level information (case name—pft in Table 1). Note that values are rounded to two significant digits after all calculations are made.
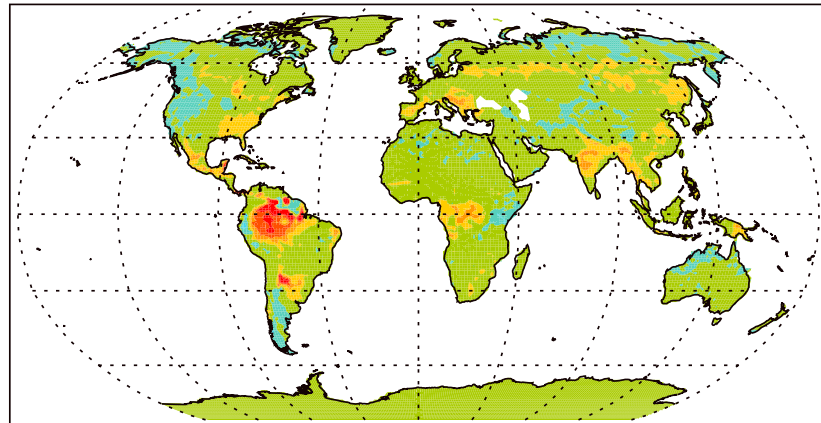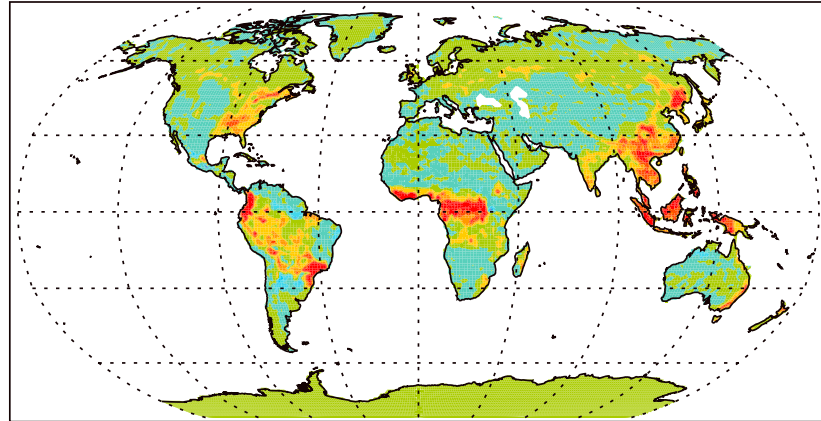
a. Land carbon losses due to climate at 2300 (kgC/m2)

b. Land carbon losses due to land use at 2300 (kgC/m2)

Figure 3. Change in land carbon at the year 2300 caused by (a) climate change from CO_2 and other anthropogenic forcing agents, and (b) human land use and land cover change, with units of kgC/m^2.

At 2300, the contribution of direct, quasi-direct, and potential indirect carbon change to the cumulative LULCC change in land carbon stock is estimated from our diagnostic model to be 39%, 17%, and 44%, respectively (Figure 4a and Table 4). Most of the land carbon change comes from the removal of tree pfts (58%), but the conversion of natural lands to harvested lands also contributes significantly (36%), while conversion of nontree pfts to crops contributes only a small amount (5%) (Figure 4a). This partitioning suggests that the indirect effects of land use conversion on carbon cycling are likely to be as large as or larger than the direct carbon changes and similar in magnitude to previous reports [*Gitz and Ciais*, 2003]. Note that in the cases without climate change, the direct and quasi-direct carbon changes are about the same as when there is climate change, but the potential indirect carbon changes are twice as large (Table 4 and Figure S3b).

As shown schematically in Figure 1, the total amount of carbon removed from the land is similar no matter when the land use conversion occurs, however, the partitioning between directly versus indirectly lost components is very sensitive to when the conversion occurs (Figure 1: blue versus red case). Using equation (5), we can calculate an amplification factor (AF) that describes how much the direct carbon fluxes due to a land conversion occurring at a particular time should be multiplied by to get the total effect of the land use conversion when integrated in time to the year 2300 (Figure 4b). Because the indirect fraction is larger for land use conversion that occurs earlier, AF is larger for conversion that occurs earlier in time (Figure 4b), decreasing from about 3.0 for clearing at 1850 to 2.4 for clearing at 2100 (when land use conversion ceases
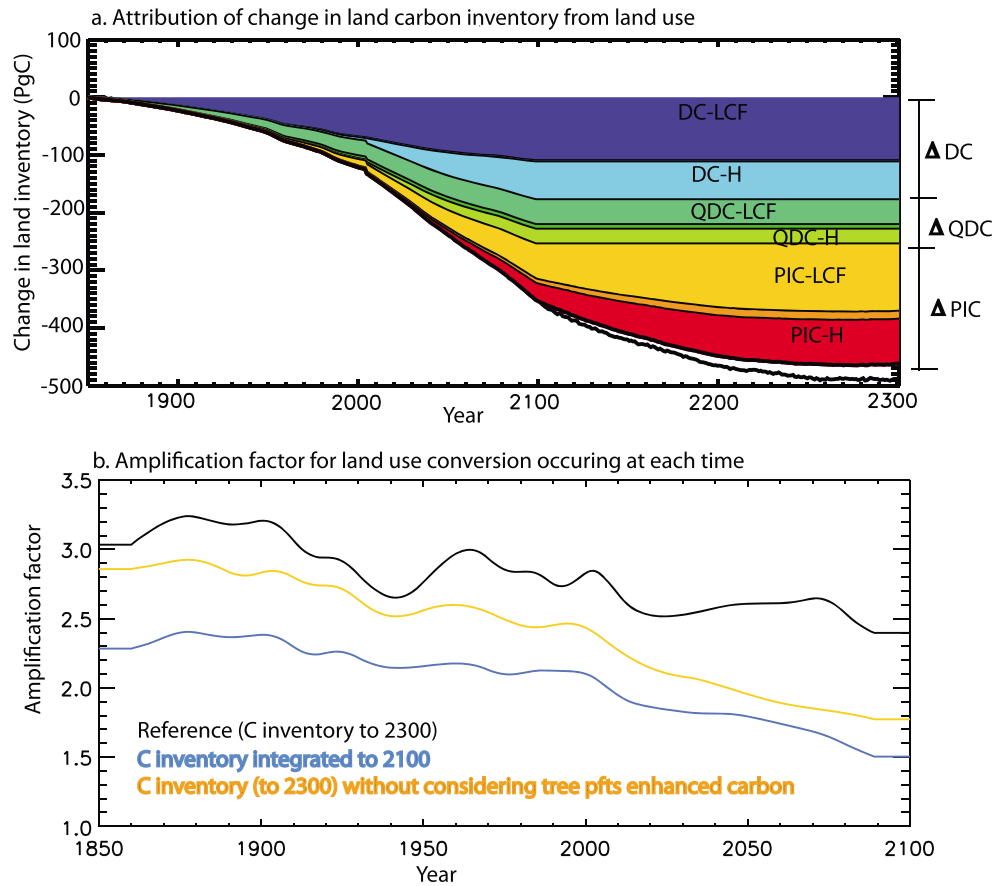
Figure 4. (a) Time series plots from 1850 to 2300 for global difference in land carbon stock from the fully coupled simulations with and without land use (e.g., difference between red solid and red dotted lines in Figure 2; blue arrow). Using equations (1–3), the relative attribution of the difference between direct carbon (DC), quasi-direct carbon (QDC), and potential indirect carbon (PIC) changes, as defined in Figure 1, is shown for three different types of processes: land conversion of forests (LCF), land conversion of nonforests (LCNF; unlabeled smaller sections between others), and harvesting (*H*). The colors represent, in order from top to bottom: DC-LCF (dark blue), DC-LCNF (blue, unlabeled small sliver), DC-H (cyan), QDC-LCF (green), QDC-LCNF (light green, unlabeled small sliver), QDC-H (chartreuse), PIC-LCF (orange), PIC-LCNF (dark orange unlabeled sliver), and PIC-H (red). The difference between the bottom black line (with LULCC minus without LUCC) and the colored regions represents the error in the estimation method (Table 4 at 2300). (b) Time series plots from 1850 to 2100 for global estimates of the amplifying factor, AF, which represents the ratio of the sum of indirect and direct carbon loss relative to the direct carbon loss for clearing at a given time step when integrated to either 2100 (blue) or 2300 (black) (equation (5)), for tree pfts where time represents the time at which land conversion took place for reference case (equation (5): reference case; black), case where tree pfts are not considered to have more carbon relative to other pfts (orange), and the case where only indirect effects through 2100 were considered (inventory integrated to 2100; blue). This panel only extends to 2100 because the simulation stops converting land at 2100. Units of Pg C.

in the model simulations conducted here). This is consistent with previous studies, which have argued that initial conditions are critical for estimating land use carbon impacts [e.g., *Goll et al.*, 2015]. Within each grid box, AF is sensitive to the model processes regulating carbon accumulation (e.g., the sensitivity of photosynthesis to rising CO_2) and the land conversion trajectory, and as a consequence these factors contribute to spatial variability in AF across continents (Figure S3a). The amplification factor tends to be slightly higher at midlatitude and high latitude than in the tropics (Figure S3c), and some of the decrease in the amplification factor with time is likely to be associated with shifts in land conversion from midlatitudes to the tropics in the RCP8.5 scenario (Figures S3a and S32c).

Previous studies considering amplification from indirect land use effects have focused on impacts through 2100 [e.g., *Gitz and Ciais*, 2003], and most CMIP5 carbon cycle analysis has focused on this time span [e.g., *Arora et al.*, 2013; *Brovkin et al.*, 2013; *Jones et al.*, 2013]. Here we show that an additional ~35% enhancement of the indirect effect of LULCC (Figure 4b; blue line versus black line) occurs when considering the changes in

Table 4. Attribution of the Change in Carbon Land Inventory Due To LULCC to Different Terms at the Year 2300[a]

Term	With Climate Change (Pg C)	Without Climate Change (Pg C)
Direct carbon (ΔDC) total	178	178
ΔDC land conversion tree pfts	111	111
ΔDC land conversion nontree pfts	2	2
ΔDC harvest	66	66
Quasi-Direct carbon (ΔQDC) total	77	77
ΔQDC land conversion tree pfts	43	43
ΔQDC land conversion nontree pfts	8	8
ΔQDC harvest	25	26
Indirect carbon (ΔIC) total	207	411
ΔIC land conversion tree pfts	117	223
ΔIC land conversion nontree pfts	14	32
ΔIC harvest	76	155
Total land conversion tree pfts (ΔDC + ΔQDC + ΔIC)	270	378
Total land conversion nontree pfts (ΔDC + ΔQDC + ΔIC)	24	43
Total harvest (ΔDC + ΔQDC + ΔIC)	167	247
Total estimated (ΔDC + ΔQDC + ΔIC)	462	668
Change in carbon inventory with LULCC minus without LULCC	488	631

[a]Terms are estimated as described in section 2.2, except for last row, which is the difference between the simulation with LULCC minus without LULCC. Here we include more significant digits to allow more detailed comparison of magnitude for the calculations. Also shown in Figure 4a (first column) and Figure S3 (second column).

the land inventory to 2300 instead of 2100, presumably because of the longer time period over which CO_2 fertilization can operate. In addition, previous studies using simple models [e.g., *Gitz and Ciais*, 2003] have not quantified the essential role of tree pfts in taking up anthropogenic CO_2 (Table 3). Here we explicitly separated the impact of tree pfts relative to other pfts (Tables 3 and S1; section 3.2) and find that the AF of tree pfts is about 20% higher than the global mean (yellow line versus black lines in Figure 4b). Thus, removal of trees is especially effective at increasing the indirect carbon flux and reducing the compatible emissions. For example, for land conversion in 2015, the amplification factor is 2.6 for trees, 2.2 for nontrees, and 1.9 if we only consider indirect effects out to the year 2100.

There are several important sources of uncertainty in the simplified approach we use to estimate the proportion of direct versus indirect carbon losses and the attribution of these losses to a specific time of conversion. First, and likely most important, are uncertainties associated with the choice of the model and scenario, which are discussed in more detail in section 4. The spatial distribution of AF (calculated for a unit of deforestation for 2015) is highly variable. As a result, estimation of the global mean AF is sensitive to the spatial structure of land use and the overlap of this pattern with spatial structure of carbon storage (Figure S5). Variations in these patterns likely would contribute to differences in global mean AF which could be calculated for different models. Comparisons between CESM (Figure S5) and other Earth system models may improve our understanding of the robustness of LULCC impacts on the terrestrial carbon budget, such as within the Land Use Model Intercomparison Project (LUMIP, http://cmip.ucar.edu/lumip). In addition, we propose a methodology here to estimate the direct, quasi-direct, and potential indirect carbon stock changes that may be of use with models that do not output these fluxes directly. This may aid with the development of a systematic approach for cross-model comparisons in LUMIP. As described in more detail in the supporting information, at individual grid cells the error associated with the approximations used here can be large, but globally averaged, the errors in the budget are approximately 15%, suggesting that the approach used here can be used to estimate the fractions of direct and indirect carbon losses associated with LULCC.

3.2. Influence of Land Use on the Carbon-Climate Feedback

Most analyses of the climate-carbon feedback have been undertaken using idealized Earth system simulations without land use change [*Arora et al.*, 2011; *Friedlingstein et al.*, 2006, 2003]. Yet both the climate-carbon feedback and LULCC are simultaneously evolving, raising questions about which set of mechanisms has a larger impact on the terrestrial carbon budget as well as possible interactions. As described above, estimating compatible emissions provides one framework for comparing the impact of these different mechanisms and demonstrates that for RCP8.5, LULCC has a considerably larger impact than
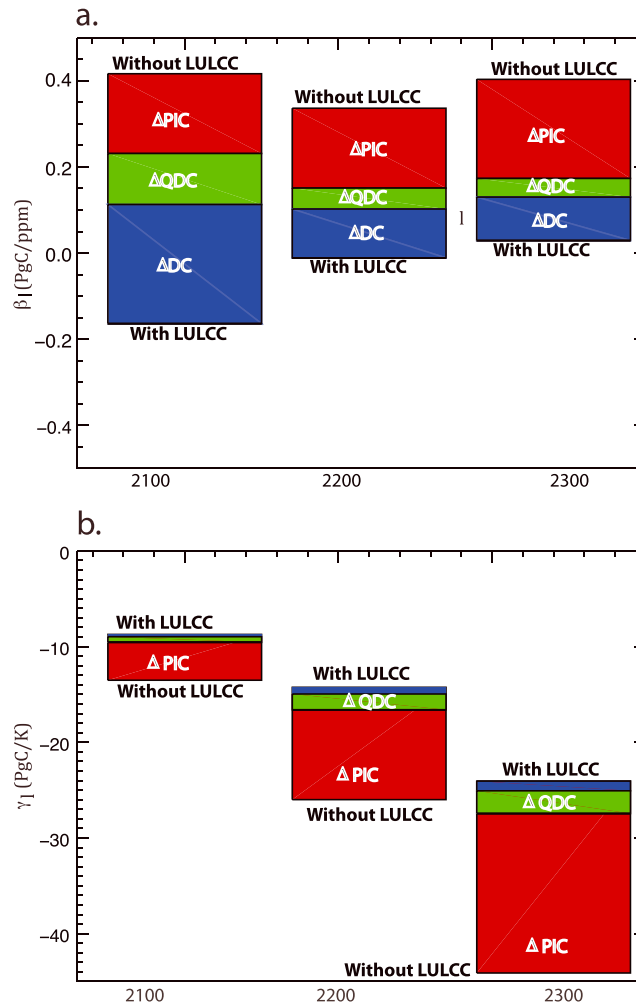
Figure 5. Bar chart showing the CO_2 impact on land carbon (a) (β_l) and the effect of temperatures on the land carbon (b) (γ_l) at three different times integrated from 1850 to 2100, 2200, or 2300. In Figure 5a the highest value is from the simulations without LULCC, and the lowest value is the run with LULCC, while in Figure 5b the most negative value is calculated in the case without LULCC (bottom of bar). The colored areas represent how much of the difference in β_l or γ_l comes from direct carbon (ΔDC; blue), quasi-direct carbon (ΔQDC; green), or potential indirect carbon (ΔPIC; red), as calculated in this paper.

the climate-carbon feedback in CESM. Another powerful conceptual framework is to assess the influence of LULCC on the gain of the carbon-climate feedback, separating the influence of LULCC on the sensitivity of the land and ocean carbon stocks to increasing atmospheric CO_2 (β_l and β_o) and the sensitivity of land and ocean carbon to increasing temperatures (γ_l and γ_o) (see the method's description in section 3.3; Figure 5). In our analysis, parameters derived from simulations with LULCC are referred to as β_l^* and γ_l^*, respectively (section 3.3; equations 8–11) and we explicitly consider the role of ΔDC, ΔQDC, and ΔPIC in modifying β_l and γ_l.

The net effect of LULCC is to reduce the gain of the carbon-climate feedback in CESM by about 10% (section 2.3), from 0.10 in 2300 to 0.09. This relatively small decrease occurs, however, as a consequence of relatively large changes in β_l and γ_l that mostly cancel each other out. As described below, LULCC decreases β_l considerably as a consequence of a loss of storage in forests, and this has the effect in equation (7) (since β_l is in the denominator) of increasing the gain of the climate-carbon feedback. However, loss of forests also means that less carbon on land is vulnerable to warming-induced losses from decreases in tropical net primary production and increases in rates of decomposition and fires. As a result, γ_l decreases in magnitude (becomes less negative). The changes in γ_l for the global biosphere has a slightly larger impact than the changes in β_l, and so the net effect is a weakening of the gain.

Without LULCC the carbon fertilization effect, β_l, is small but positive over most of the simulation (Figure 5a, top of the bars). When simulations include LULCC, β_l^* becomes negative (Figure 5a, bottom of the bars), due to a combined impact of ΔDC, ΔQDC, and ΔPIC (Figure 5a, colored areas). The sensitivity of land carbon to increasing temperatures for the case without LULCC, γ_l, increases in negative magnitude with time (Figure 5b, bottom of the bars). When LULCC is included, this increase in magnitude is reduced (top of the bars), almost exclusively due to ΔPIC. This is consistent with the budgets at 2300 (Table 4), indicating a very similar estimate of ΔDC and ΔQDC in the simulations including or excluding climate change.

The sensitivity of land carbon uptake to atmospheric CO_2, β_l, shows the strongest positive response in the Amazon and some parts of Asia (Figure S5a). The impact of including LULCC is negative almost everywhere (Figure S6b), consistent with the switch in the global average β_l term from positive to negative when LULCC is

included (Figure 5a). On the other hand, the sensitivity of land carbon to increasing temperature, γ_l, is negative almost everywhere (Figure S7a), while the inclusion of LULCC has a positive effect (Figure S7b), dampening out the impact of climate change on terrestrial carbon losses (Figure S7b). As discussed above (section 3.1), most of the impact of LULCC on β_l and γ_l occur in the tree pfts (Table 3), and thus, the removal of trees during deforestation or harvest causes a decrease in carbon concentration and carbon-climate feedbacks.

Including or excluding LULCC also changes the relative importance of land and ocean contributions to the climate-carbon feedback. With LULCC, γ_o is larger than γ_l*, especially after 2100 [*Randerson et al.*, 2015]. However, when LULCC is excluded γ_l is more negative, and γ_l and γ_o have a similar magnitude by the end of the simulation (Figure 5b, contrast with *Randerson et al.* [2015]). Similarly, β_l* is smaller than β_l, and indeed almost zero, and thus much smaller than β_o.

4. Discussion and Conclusions

Here we present the first estimates of the impact of LULCC on multicentennial changes in terrestrial carbon storage and interactions with carbon cycle feedbacks using a full-complexity Earth system model. By 2100, LULCC and the land contribution to the climate-carbon feedback reduce cumulative compatible emissions estimated in CESM by 350 and 40 Pg C, respectively, while by 2300, these values increase to 490 and 230 Pg C (Table 2 and Table 3). Much of the uptake of anthropogenic carbon in these simulations occurs in tree pfts, highlighting the importance of forests in potentially modifying atmospheric CO_2.

The proportion of the change in the land carbon inventory that is not directly emitted as a part of the land use carbon flux tends to increase with the time since clearing [e.g., *Gasser and Ciais*, 2013, *Gitz and Ciais*, 2003; *Hansis et al.*, 2015; *Pongatz et al.*, 2009]. In our simulations with RCP8.5, the indirect carbon inventory (the sum of the ΔQDC and ΔPIC, section 2.2) is over 60% of the total LULCC flux by 2300, illustrating the multicentury carbon cycle legacy of land use decisions made during the next several decades.

We report amplification factors that describe the enhancement of direct land conversion of carbon by the indirect land carbon flux in the Earth system model simulations extending to 2300 and show that these factors vary as a function of the time of land conversion. This study suggests that current (2016) land use conversion from natural forests to harvested lands contributes an additional 160% (AF = 2.6) through indirect carbon effects out to 2300. (Figure 4b). Overall, the model indicates a global average amplification factor (AF) of 3.0 from land conversion in 1865, 2.6 in 2015, and 2.4 in 2100. Our results suggest that considering the evolution of the Earth system to the year 2300 increases the amplification factor by approximately 35%, compared with a 2100 time horizon. Because tree pfts are responsible for much of the enhanced uptake from 1850 to 2100 (section 3.1; Table 3), deforestation is particularly important, and excluding trees reduces AF by 20%.

LULCC also changes the sensitivities of land carbon stocks to increasing atmospheric CO_2 and temperature, and thus the gain of the carbon-climate feedback [*Arora et al.*, 2013; *Friedlingstein et al.*, 2006]. The dominant impact on the gain from LULCC is from the loss of tropical forests, which reduces the sensitivity of terrestrial carbon stocks to temperature increases and drying. Estimates of β_l* are sensitive to both the direct and indirect carbon inventory changes, while γ_l* is predominantly impacted by the indirect carbon inventory changes.

Our findings are likely to be sensitive to both the details of the land carbon model [*Thornton et al.*, 2009] and the future scenario used (here RCP8.5 [*Hurtt et al.*, 2011; *Lawrence et al.*, 2012b]), as well as the physical climate simulation [*Hurrell et al.*, 2013]. CESM includes nitrogen limitation of gross primary production and thus has a weaker response of photosynthesis to CO_2 fertilization and less uptake of CO_2 in natural lands as compared with other CMIP5 models [*Arora et al.*, 2013; *Jones et al.*, 2013; *Thornton et al.*, 2009] and some observations [*Friedlingstein and Prentice*, 2010]. The relatively low sensitivity of CESM to rising CO_2 suggests that our calculations may underestimate the indirect carbon fluxes associated with LULCC. This is consistent with the higher amplification factors deduced in simulations extending to 2100 as reported in *Gitz and Ciais* [2003] for different land use scenarios using a model with a stronger response of photosynthesis to CO_2 fertilization. On the other hand, the CESM model tends to have a lower temperature sensitivity of land and ocean carbon uptake [*Arora et al.*, 2013; *Jones et al.*, 2013] and thus may lose less carbon due to temperature increases, especially after 2100. Because the physical parameterizations of the Earth system model and the land use scenario

are important to the impact of LULCC and the calculation of AF, calculating these values across multiple models provide one means to assess the robustness of these results. The simple calculations used here (equations 1–5) could be applied using idealized no LULCC simulations as part of the proposed Land Use Model Intercomparison Project, for example [e.g., http://cmip.ucar.edu/lumip].

The land use conversion and harvesting rates used here and in the CMIP5 tend to underestimate current deforestation rates and are optimistic that future deforestation rates will be lower than current rates [*Ciais et al.*, 2013b; *van Vuuren et al.*, 2011; *Ward et al.*, 2014], so it is likely that the simulations underestimate rates of forest loss. The harvesting rates used here are higher than estimated in the forcing data, which might make up for the low land use conversion rates (section 2.1; [*Hurtt et al.*, 2011; *Lawrence et al.*, 2012b]), although this difference could also be due to differences in methodology [e.g., *Hansis et al.*, 2015]. In any case, the results here suggest that carbon feedbacks in coupled models are quite sensitive to the LULCC time series prescribed in a particular scenario. This result compliments previous studies highlighting the importance of the initial carbon amounts, parameterization details, and methodological choices for carbon cycle impacts of LULCC [e.g., *Goll et al.*, 2015; *Hansis et al.*, 2015]. We are also attempting to simulate a process that occurs at a much finer resolution using $1° \times 1°$ grid boxes, which is unlikely to capture important interactions—contributing to additional uncertainties. Recent studies also highlight the importance of carbon losses from agricultural management of soils, a process that is not well represented in these simulations [*Levis et al.*, 2014; *Pugh et al.*, 2015].

Integrated assessment models (IAM) are used to predict the land use conversion for agriculture and pasture that is subsequently applied to full Earth system model simulations. IAMs used in the construction of the RCP scenarios assume that the continued increases in agricultural yield due to improved management, technology, and economic growth will reduce the rate of deforestation in the future, despite increases in population and shifts in diet [*Riahi et al.*, 2011; *Riahl et al.*, 2007; *van Vuuren et al.*, 2011]. The combined historical and RCP8.5 estimates of current deforestation rates are less than those observed during the past two decades based on Food and Agriculture Organization estimates [*Food and Agriculture Organization*, 2010; *Hurtt et al.*, 2011; *Meyfroidt and Lambin*, 2011], though more recent satellite estimates suggest even larger deforestation rates [*Hansen et al.*, 2013]. While the future yield projections are very sensitive to assumptions about the ability of humans to innovate both agricultural management methods and crop genetic attributes [e.g., *Fischer et al.*, 2005], some evidence suggests that yield improvements may already be decreasing [*Ray et al.*, 2012] and that agricultural crops may be more sensitive to temperature than previously estimated [*Lobell et al.*, 2011]. On the other hand, estimates of net primary production and respiration in Earth system models assume a static response to temperature [e.g., *Oleson et al.*, 2010], although there is evidence that plants can acclimate to higher temperatures on seasonal and interannual timescales [*Kattge and Knorr*, 2007; *Atkin et al.*, 2008; *Sendall et al.*, 2015]. This is consistent with other evidence that Earth system models may be overly pessimistic about the impact of higher temperatures on land carbon [*Frank et al.*, 2010; *Keenan et al.*, 2013; *Mahecha et al.*, 2010], and studies which include temperature acclimation indicate that including the effects of acclimation would increase the terrestrial carbon in Earth system models [*Arneth et al.*, 2012; *Atkin et al.*, 2008; *King et al.*, 2006]. Thus, the IAM models used to predict future land use conversion may be underestimating the threat to forests from deforestation, while Earth system models may be overestimating the threat to forests from higher temperatures. Future studies should consider in more detail the inconsistency in treatment of temperature on terrestrial ecosystems and the implications for LULCC and terrestrial carbon.

As a final consideration, we note that the results of this study are sensitive to the choice of the future scenario (RCP8.5). The deforestation in all the RCPs is lower than current Food and Agriculture Organization or satellite-based estimates [*Ward et al.*, 2014], although the RCP8.5 has the highest deforestation rates. Since current emissions and emission trends of CO_2 have been higher than estimated in the RCP8.5 [*Friedlingstein et al.*, 2014], this scenario remains plausible and thus important to consider. Additionally, the time to stabilization of atmospheric CO_2 is longest for the RCP8.5 compared to the other RCPs [*van Vuuren et al.*, 2011], and thus the longer timescales are most important to consider for RCP8.5. If one considers shorter timescales (i.e., only to 2100), other constituents besides CO_2 become more important, and the radiative forcing associated with LULCC is twice that of fossil fuel and other anthropogenic emissions, per unit of CO_2 directly emitted [*Ward et al.*, 2014]. This is because on shorter timescales, warming by fossil fuel emitted

CO$_2$ is partially offset by contemporaneous aerosol emissions that tend to cool, while LULCC emissions of CO$_2$ are augmented in their warming by LULCC emissions of methane and nitrous oxide emissions [*Ward et al.*, 2014]. Overall, this means that on the short to medium timescales (out to 2100), emissions of CO$_2$ from LULCC lead to twice the warming as emissions from other sources [*Ward et al.*, 2014]. Here we show that on longer timescales, if humans continue toward RCP8.5 (or higher) CO$_2$ levels, direct LULCC CO$_2$ emissions will be significantly augmented by indirect LULCC emissions, and again direct LULCC CO$_2$ emissions will cause more warming than fossil fuel CO$_2$ emissions by a factor of 2–3. While fossil fuel emissions of CO$_2$ will drive future climate warming [*Allen et al.*, 2009; *van Vuuren et al.*, 2011] and must remain the emphasis of policy makers, this study suggests that protection of natural forested lands could be an effective method of reducing CO$_2$ concentrations.

References

Allen, M., D. Frame, C. Huntingford, C. Jones, J. A. Lowe, M. Meinshausen, and N. Meinshausen (2009), Warming caused by the cumulative carbon emissions towards the trillionth tonne, *Nature*, *458*, 1163–1166, doi:10.1038/nature08019.

Archer, D., et al. (2009), Atmospheric lifetime of fossil fuel carbon dioxide, *Annu. Rev. Earth Planet. Sci.*, *37*, 117–134.

Arneth, A., L. Mercado, J. Kattge, and B. Booth (2012), Future challenges of representing land-processes in studies on land-atmosphere interactions, *Biogeosciences*, *9*, 3587–3599.

Arora, V. K., et al. (2011), Carbon emission limits required to satisfy future representative concentration pathways of greenhouse gases, *Geophys. Res. Lett.*, *38*, L05805, doi:10.1029/02010GL046270.

Arora, V. K., et al. (2013), Carbon-concentration and carbon-climate feedbacks in CMIP5 Earth system models, *J. Clim.*, *26*, 5289–5314.

Atkin, O., et al. (2008), Using temperature-dependent changes in leaf scaling relationships to quantitatively account for thermal acclimation of respiration in a coupled global climate-vegetation model, *Global Change Biol.*, *14*, 2709–2726, doi:10.1111/j.1365-2486.2008.01664.x.

Bonan, G. (2008), Forests and climate change: Forcings, feedbacks and the climate benefits of forests, *Science*, *320*, 1444–1448, doi:10.1126/science.1155121.

Boucher, O., P. Halloran, E. Burke, M. Doutriaux-Boucher, C. D. Jones, J. Lowe, M. A. Ringer, E. Robertson, and P. Wu (2012), Reversibility in an Earth system model in response to CO$_2$ concentration changes, *Environ. Res. Lett.*, *7*, doi:10.1088/1748-9326/1087/1082/024013.

Brovkin, V., et al. (2013), Effect of anthropogenic land-use and land-cover changes on climate and land carbon storage in CMIP5 projections for the twenty-first century, *J. Clim.*, *26*, 6859–6881, doi:10.1175/JCLI-D-6812-00623.00621.

Ciais, P., T. Gasser, J. Paris, K. Caldeira, M. R. Raupach, J. Canadell, A. Patwardhan, P. Friedlingstein, S. Piao, and V. Gitz (2013a), Attributing the increase in atmospheric CO$_2$ to emitters and absorbers, *Nature Clim. Change*, *3*, 926–930.

Ciais, P., et al. (2013b), Carbon and other biogeochemical cycles, in *Climate Change 2013: The Physical Science Basis. Contribution of Working Group I to the Fifth Assessment Report of the Intergovernmental Panel on Climate Change*, edited by T. Stocker, Cambridge Univ. Press, Cambridge, U. K.

Danabasoglu, G., S. Bates, B. Briegleb, S. R. Jayne, M. Jochum, W. G. Large, S. Peacock, and S. G. Yeager (2012), The CCSM4 ocean component, *J. Clim.*, *25*, 1361–1389, doi:10.1175/jcli-d-1311-00091.00091.

Denoblet-Ducoudre, N., et al. (2012), Determining robust impacts of land-use-induced land cover changes on surface climate over North America and Eurasia: Results from the first set of LUCID experiments, *J. Clim.*, *25*, 3261–3281, doi:10.1175/JCLI-D-3211-00338.00331.

Food and Agriculture Organization (2010), *Global Forest Resources Assessment*, FAO, Rome.

Feddema, J., K. Oleson, G. Bonan, L. Mearns, L. Buja, G. Meehl, and W. Washington (2005), The importance of land-cover change in simulating future climates, *Science*, *310*, 1674–1678.

Fischer, G., M. Shah, F. Tubiello, and H. Van Velhuizen (2005), Socio-economic and climate change impacts on agriculture: An integrated assessment, 1990–2080, *Philos. Trans. R. Soc.*, *360B*, 2067–2083, doi:10.1098/rstb.2005.1744.

Foley, J., et al. (2005), Global consequences of land use, *Science*, *309*, 570–574.

Frank, D., J. Esper, C. Raible, U. Buntgen, V. Trouet, B. D. Stocker, and F. Joos (2010), Ensemble reconstruction constraints on the global carbon cycle sensitivity to climate, *Nature*, *463*, 527–531, doi:10.1038/nature08769.

Friedlingstein, P., and C. Prentice (2010), Carbon-climate feedbacks: A review of model and observation based estimates, *Curr. Opin. Environ. Sustain.*, *2*, 251–257.

Friedlingstein, P., J.-L. Dufresne, P. M. Cox, and P. Rayner (2003), How positive is the feedback between climate change and the carbon cycle?, *Tellus*, *55B*, 692–700.

Friedlingstein, P., et al. (2006), Climate-carbon cycle feedback analysis, results from the C4MIP model intercomparison, *J. Clim.*, *19*, 3337–3353.

Friedlingstein, P., et al. (2014), Persistent growth of CO$_2$ emissions and implications for reaching climate targets, *Nat. Geosci.*, *7*, 709–715.

Frolicher, T. L., and F. Joos (2010), Reversible and irreversible impacts of greenhouse gas emissions in multi-century projections with the NCAR global coupled carbon cycle-climate model, *Clim. Dyn.*, *35*, 1439–1459, doi:10.1007/s00382-00009-00727-00380.

Gasser, T., and P. Ciais (2013), A theoretical framework for the net land-to-atmosphere CO$_2$ flux and its implications in the definition of "emissions from land-use change", *Earth Syst. Dyn.*, *4*, 171–186, doi:10.5194/esd-5194-5171-2013.

Gitz V., Ciais P. (2003), Amplifying effects of land-use change on future atmospheric CO$_2$ levels, *Global Biogeochem. Cycles*, *17*(1), 1024; doi:10.1029/2002GB001963.

Goll, D., V. Brovkin, J. Liski, T. Raddatz, T. Thum, and K. Todd-Brown (2015), Strong dependence of CO$_2$ emissions from anthropogenic land cover change on initial land cover and soil carbon parametrization, *Global Biogeochem. Cycles*, *29*, 1511–1523, doi:10.1002/2014GB004988.

Hansen, M., et al. (2013), High-resolution global maps of 21st century forest cover change, *Science*, *342*, doi:10.1126/science./1244693.

Hansis, E., S. Davis, and J. Pongratz (2015), Relevance of methodological choices for accounting of land use change carbon fluxes, *Global Biogeochem. Cycles*, *29*, 1230–1246, doi:10.1002/2014GB004997.

Heald C., and D. Spracken (2015), Land use change impacts on air quality and climate, *Chem. Rev.*, *115*(10), 4476–4496, doi:10.1021/cr500446g.

Houghton, R. (2003), Revised estimates of the annual net flux of carbon to the atmosphere from changes in land use and land management 1850–2000, *Tellus*, *55B*, 378–390.

Hurrell, J. W., et al. (2013), The community Earth system model: A framework for collaborative research, *Bull. Am. Meteorol. Soc.*, doi:10.1175/BAMS-D-1112-00121.

Hurtt, G. C., et al. (2011), Harmonization of land-use scenarios for the period 1500–2100: 600 years of global gridded annual land-use transitions, wood harvest, and resulting secondary lands, *Clim. Change*, *109*, 117–161, doi:10.1007/s10584-0011-10153-10582.

Jackson, R. B., et al. (2008), Protecting climate with forests, *Environm. Res. Lett.*, *3*, doi:10.1088/1748-9326/1083/1084/044006.

Jones, C., et al. (2013), 21st century compatible CO_2 emissions and airborne fraction simulated by CMIP5 Earth system models under 4 Representative Concentration Pathways, *J. Clim.*, *26*, 4398–4413, doi:10.1175/JCLI-D-4312-00554.00551.

Kattge, J., and W. Knorr (2007), Temperature acclimation in a biochemical model of photosynthesis: A reanalysis of data from 36 species, *Plant, Cell Environ.*, *30*, 1176–1190.

Keenan, T., D. Hollinger, G. Bohrer, D. Dragoni, J. Munger, H. Schmid, and A. Richardson (2013), Increase in forest water-use efficiency as atmospheric carbon dioxide concentrations rise, *Nature*, *499*, doi:10.1028/nature12291.

Keppel-Aleks, G., et al. (2013), Evolution of atmospheric carbon dioxide variability during the 21st century in a coupled carbon-climate model, *J. Clim.*, *26*, doi:10.1175/JCLI-D1112-00589.00581.

King, A., C. Gunderson, W. Post, D. Weston, and S. Wullschleger (2006), Plant respiration in a warmer world, *Science*, *312*, 536–537.

Lamarque, J. F., G. P. Kyle, M. Meinshausen, K. Riahi, S. J. Smith, D. P. van Duren, A. J. Conley, and F. Vitt (2011), Global and regional evolution of short-lived radiatively-active gases and aerosols in the Representative Concentration Pathways, *Clim. Change*, *109*, 191–212.

Lamarque, J.-F., et al. (2010), Historical (1850–2000) gridded anthropogenic and biomass burning emissions of reactive gases and aerosols: Methodology and application, *Atmos. Chem. Phys.*, *10*, 7017–7039.

Lawrence, D. M., K. W. Oleson, M. G. Flanner, C. G. Fletcher, P. Lawrence, S. Levis, S. Swenson, and G. B. Bonan (2012a), The CCSM4 land simulation, 1850-2005: Assessment of surface climate and new capabilities, *J. Clim.*, *25*, 2240–2260.

Lawrence, P., et al. (2012b), Simulating the biogeochemical and biogeophysical impacts of the transient land cover change and wood harvest in the Community Climate System Model [CCSM4] from 1850 to 2100, *J. Clim.*, *25*, 3071–3095.

Lequere, C., et al. (2009), Trends in the sources and sinks of carbon dioxide, *Nat. Geosci.*, *2*, 1831–1836, doi:10.1038/ngeo1689.

Levis, S., M. Hartman, and G. Bonan (2014), The Community Land Model underestimates land-use CO_2 emissions by neglecting soil disturbance from cultivation, *Geosci. Model Dev.*, *7*, 613–620, doi:10.5194/gmd-5197-5613-2014.

Lindsay, K., G. Bonan, S. Doney, F. M. Hoffman, D. M. Lawrence, M. C. Long, N. M. Mahowald, K. J. Moore, J. T. Randerson, and P. E. Thornton (2014), Preindustrial and 20th century experiments with the Earth system model CESM1-[BGC], *J. Clim.*, *27*, 8981–9005.

Lobell, D., W. Schlenker, and J. Costa-Roberts (2011), Climate trends and global crop production since 1980, *Science*, *333*, 616–620.

Long, M. C., K. Lindsay, S. Peacock, J. K. Moore, and S. C. Doney (2013), Twentieth-century oceanic carbon uptake and storage in CESM1[BGC], *J. Clim.*, *26*, 6775–6800, doi:10.1175/jcli-d-6712-00184.00181.

Macdougall, A., C. Avis, and A. Weaver (2012), Significant existing commitment to warming from the permafrost carbon feedback, *Nat. Geosci.*, *5*, 719–721, doi:10.1038/NGEO1573.

Mahecha, M., et al. (2010), Global convergence in the temperature sensitivity of respiration at ecosystem level, *Science*, *329*, doi:10.1126/science.1189587.

Meehl, G., et al. (2013), Climate system response to external forcings and climate change projections in CCSM4, *J. Clim.*, *11*, 3661–3683, doi:10.1175/Jcl-d-3611-00240.00241.

Meinshausen, M., et al. (2011), The RCP greenhouse gas concentrations and their extensions from 1765 to 2300, *Clim. Change*, doi:10.1007/s10584-0011-10156-z.

Meyfroidt, P., and E. Lambin (2011), Global forest transition: Prospects for an end to deforestation, *Annu. Rev. Environ. Resour.*, *36*, 343–371, doi:10.1146/annurev-environ-090710-143732.

Moore, J. K., K. Lindsay, S. Doney, M. Long, and K. Misumi (2013), Marine ecosystem dynamics and biogeochemical cycling in the Community Earth System Model1 [BGC]: Comparison of the 1990s with the 2090s under the RCP4.5 and RCP8.5 scenarios, *J. Clim.*, *26*, 9291–9312, doi:10.1175/jcli-d-9212-00566.00561.

Myhre, G., et al. (2013), Anthropogenic and natural radiative forcing, in *Climate Change 2013: The Physical Science Basis. Contribution of Working Group I to the Fifth Assessment Report of the Intergovernmental panel on Climate Change*, edited by T. Stocker et al., Cambridge Univ. Press, Cambridge, U. K.

Neale, R., J. Richter, S. Park, P. Lauritzen, S. Vavrus, P. Rasch, and M. Zhang (2013), The mean climate of the Community Atmosphere Model (CAM4) in forced SST and fully coupled experiments, *J. Clim.*, *26*, 5150–5168, doi:10.1175/jcli-d-5112-00236.00231.

Oleson, K. W., et al. (2010), Technical description of version 4.0 of the Community Land Model, *NCAR Technical Note*, Boulder, Colo.

Oleson, K., et al. (2013), Technical description of version 4.5 of the Community Land Model (CLM), *NCAR Technical Note*, Boulder, Colo.

Pongatz, J., C. Reick, T. Raddatz, and M. Claussen (2009), Effects of anthropogenic land cover change on the carbon cycle of the last millennium, *Global Biogeochem. Cycles*, *23*, GB4001, doi:10.1029/2009GB003488.

Pongatz, J., C. Reick, T. Raddatz, and M. Claussen (2010), Biogeophysical versus biogeochemical climate response to historical anthropogenic land cover change, *Geophys. Res. Lett.*, *37*, L08702, doi:10.1029/2010GL043010.

Pugh, T., A. Arneth, S. Olin, A. Ahlstrom, A. Bayer, K. Klein Goldewijk, M. Lindeskog, and G. Schurgers (2015), Simulated carbon emissions from land-use change are substantially enhanced by accounting for agricultural management, *Environ. Res. Lett.*, *10*, 124008, doi:10.1210/121748-129326/124010/124012/124008.

Randerson, J. T., K. Lindsay, M. E. Weiwei Fu, F. Hoffman, J. K. Moore, N. Mahowald, and S. Doney (2015), Multi-century changes in ocean and land contributions to climate-carbon feedbacks, *Global Biogeochem. Cycles*, *29*, 744–759, doi:10.1002/2014GB005079.

Ray, D. K., N. Ramankutty, N. D. Mueller, P. C. West, and J. A. Foley (2012), Recent patterns of crop yield growth and stagnation, *Nat. Commun.*, *3*, 1293.

Riahi, K., S. Rao, V. Krey, C. Cho, V. Chirkov, G. Fischer, G. Kindermann, N. Nakicenovic, and P. Rafaj (2011), RCP 8.5—A scenario of comparatively high greenhouse gas emissions, *Clim. Change*, *109*, 33–57, doi:10.1007/s10584-0011-10149-y.

Riahl, K., A. Gruebler, and N. Nakicenovic (2007), Scenarios of long-term socio-economic and environmental development under climate stabilization, *Technol. Forecast. Social Change*, *74*, 887–935.

Sendall, K. M., P. B. Reich, C. Zhao, H. Jihua, X. Wei, A. Stefanski, K. Rice, R. L. Rich, and R. A. Montgomery (2015), Acclimation of photosynthetic temperature optima of temperate and boreal tree species in response to experimental forest warming, *Global Change Biol.*, *21*, 1342–1357.

Swann, A. L. S., F. M. Hoffmann, C. D. Koven, and J. T. Randerson (2016), Plant responses to increasing CO_2 reduce estimates of climate impacts on drought severity, *Proc. Natl. Acad. Sci. U.S.A.*, doi:10.1073/pnas.1604581113.

Taylor, K. E., R. J. Stouffer, and G. A. Meehl (2009), A summary of the CMIP5 experimental design. [Available at http://cmip-pcmdi.llnl.gov/cmip5/docs/Taylor_CMIP5_design.pdf.]

Thornton, P., S. Doney, K. Lindsay, J. K. Moore, N. Mahowald, J. T. Randerson, I. Fung, J.-F. Lamarque, J. J. Feddema, and Y.-H. Lee (2009), Carbon-nitrogen interactions regular climate-carbon cycle feedbacks: Results from an atmosphere-ocean general circulation model, *Biogeosciences*, *6*, 2099–2120, doi:10.5194/bg-2095-2099-2009.

Todd-Brown, K., J. Randerson, W. Post, F. Hofffman, C. Tarnocai, E. Schnuur, and S. Allison (2013), Causes of the variation in soil carbon simulations from CMIP5 Earth system models and comparison with observations, *Biogeosciences*, *10*, 1717–1736, doi:10.5194/bg-1710-1717-2013.

Unger, N. (2014), Human land-use driven reduction of forest volatiles cools global climate, *Nat. Clim. Change*, doi:10.1038/nclimate2347.

Van Vuuren, D. P., et al. (2011), The representative concentration pathways: An overview, *Clim. Change*, *109*, 5–31.

Ward, D. S., N. Mahowald, and S. Kloster (2014), Potential climate forcing of land use and land cover change, *Atmos. Chem. Phys.*, *14*, 12,701–12,724.